Infrared Surface Plasmon Resonance: A Novel Tool for Real Time Sensing of Variations in Living Cells

Roy Ziblat,* Vladislav Lirtsman,* Dan Davidov,* and Benjamin Aroeti†

*Racah Institute of Physics and †Department of Cell and Animal Biology, The Alexander Silberman Institute of Life Sciences, The Hebrew University of Jerusalem, Jerusalem 91904, Israel

ABSTRACT We developed a novel surface plasmon resonance (SPR) method, based on Fourier transform infrared (FTIR) spectroscopy, as a label-free technique for studying dynamic processes occurring within living cells in real time. With this method, the long (micrometer) infrared wavelength produced by the FTIR generates an evanescent wave that penetrates deep into the sample. In this way, it enables increased depth of sensing changes, covering significant portions of the cell-height volumes. HeLa cells cultivated on a gold-coated prism were subjected to acute cholesterol enrichment or depletion using cyclodextrins. Cholesterol insertion into the cell plasma membrane resulted in an exponential shift of the SPR signal toward longer wavelengths over time, whereas cholesterol depletion caused a shift in the opposite direction. Upon application of the inactive analog α-cyclodextrin (α-CD), the effects were minimal. A similar trend in the SPR signal shifts was observed on a model membrane system. Our data suggest that FTIR-SPR can be implemented as a sensitive technique for monitoring in real time dynamic changes taking place in living cells.

INTRODUCTION

Real time monitoring of dynamic processes at the surface of living cells is an approach that has gained increased popularity in recent years, and it certainly holds promise in unraveling some of the mysteries of modern cell biology in the next decade. Surface plasmon resonance (SPR) operating within the visible wavelength (e.g., BIAcore) was introduced commercially only in the past few years but is now recognized as a valuable tool for monitoring in real time the interactions between diverse biomolecules (1–3). However, the system is based on studying the interactions between two components (e.g., soluble proteins) while one is attached to the surface of a gold-coated sensor chip. Hence, this technology is not well suited for studying interactions in situ or in vivo, and the characteristics of the in vitro interactions detected by the current SPR techniques may not be relevant to those interactions taking place within living cells. This therefore precludes the use of the SPR method to study interactions in live cells.

Cells display specific abilities to interact with each other and with various molecules of life (proteins, lipids, etc.). It is believed that the extreme complexity and diversity of cell architecture and function is largely attributed to the properties of these interactions. Given the limitations of SPR within the visible wavelength, it is therefore essential to develop a new experimental strategy capable of monitoring quantitatively in real time the dynamic interactions between biomolecules and their cognate receptors in cells. In the framework of this endeavor, we have recently developed a novel SPR method based on Fourier transform infrared FTIR-SPR, operating in the near infrared (IR) wavelength range (typically 0.8–5 μm, although here we show results for up to 2 μm). This FTIR-SPR system possesses several important inherent advantages over the traditional BIAcore technique for which it may be considered superior for studying cells. Unlike SPR in the visible wavelength, the IR wavelength used for FTIR-SPR produces an evanescent wave that penetrates deep into the sample (up to ~10 μm, depending upon the IR wavelength used to excite the sample), thus allowing, in principle, SPR to be measured with a greater sensitivity to significant regions within the cell's volume. Moreover, in contrast to the photodamage potentially induced by cell radiation in the visible light range, cells and other biological specimens are practically transparent upon exposure to IR radiation. Therefore, IR radiation used in the FTIR-SPR experiments cannot cause photodamage and phototoxicity to the living material.

Cholesterol, a lipid belonging to the steroid group, is an extremely important constituent of cellular membranes. Although the precise level of the lipid varies between different cell types, cholesterol is present ubiquitously at 20–40 mol % of plasma membrane lipids in all eukaryotic cells (4,5). Importantly, it plays a pivotal role in a wide range of physiological and pathophysiological processes, some of which are thought to be mediated by cholesterol- and sphingolipid-rich ''raft'' microdomains (for recent reviews, see Simons and Ikonen (6), Mouritsen and Zuckermann (7), Barenholz (8), and Holthuis and Levine (9)). Cholesterol has also been shown to modulate the membrane's biophysical properties. For example, under certain conditions, its insertion into simple model membranes caused an increase in lipid packaging and bilayer thickness (10–12). However, recent studies have suggested that cholesterol's ability to modulate bilayer thickness of native cell membranes might be less pronounced (13).

Submitted August 5, 2005, and accepted for publication December 12, 2005.

Address reprint requests to Benjamin Aroeti, Tel.: 972-2-6585915; Fax: 972-2-6584547; E-mail: aroeti@cc.huji.ac.il; or Dan Davidov, Tel.: 972-2-6585915; Fax: 972-2-5617805; E-mail: davidov@vms.huji.ac.il.

0006-3495/06/04/2592/08 $2.00

doi: 10.1529/biophysj.105.072090

SPR measurements are highly sensitive to both the thickness and dielectric properties of layers (14). This property should in principle allow a more sensitive detection of changes in membrane bilayer dielectric and thickness by FTIR-SPR in response to altered membrane cholesterol levels. To explore this hypothesis, we performed FTIR-SPR measurements on viable cells and model phospholipid membranes whose membrane cholesterol contents had been manipulated by cyclodextrin treatment. To the best of our knowledge, this is the first time that evidence has been presented regarding the ability of FTIR-SPR to detect online and in a time-dependent manner specific changes occurring in cell membrane cholesterol levels. Thus, the development of FTIR-SPR shows great potential as a valuable label-free method to study in real time a variety of interactions in the membranes of living cells.

MATERIALS AND METHODS

The FTIR-SPR system

The experimental setup operating in the range of 0.8–2 μm is schematically depicted in Fig. 1, upper panel. It is based on a SF-11 glass right angle prism in the Kretschmann configuration equipped with a Bruker Equinox 55 FTIR spectrometer (Bruker Optik GmbH, Ettlingen, Germany) as an IR source. It is fully computer controlled and can directly measure the SPR versus the wavelength at constant incident angles. The setup includes a beam collimation system with a beam divergence of 0.19°; the specimen is illuminated by a beam whose diameter is 10 mm. The beam collimation is produced by a pair of BK-7 lenses, L1 and L2 (with 62.9 and 150 mm focal lengths, respectively), and a 0.5 mm pinhole located in between. A third BK-7 lens, L3 ($D = 25$ mm, focal length of 62.9 mm), focuses the beam into the InGaAs (D427) IR detector. The prism and detector are mounted onto a θ-2θ Huber goniometer with an angular precision of $\pm 0.001°$. The base of the prism was coated with a 25–35 nm thick gold film using the electron-beam evaporation technique. The film's thickness for each experiment was chosen in such a way that the SPR in the 0.8–1.9 μm range could be detected sensitively. We used a specialized flow chamber (Bioanalytical System, West Lafayette, IN) with two holes to allow inlet and outlet liquid flow. The solution was injected into the chamber at a suitable flow rate using a motorized bee syringe pump with a variable speed controller. The flow chamber is attached to the metal-coated prism so that the solution that filled the chamber was in direct contact with the metal film (and the biological sample attached to it). All measurements were performed at 37°C $\pm$ 0.1°C. The SPR phenomenon is highly sensitive to dielectric alterations contributed by small fluctuations in solute concentration, temperature, and other factors. All these effects were carefully subtracted from the data in each experiment. We used the mβCD as an agent to manipulate cholesterol levels in cells and artificial phospholipid monolayers (see below). Before its application on cells or phospholipid monolayers, it was essential to establish its background binding capacity to the bare gold surface. Experiments in which the gold surface alone was exposed to the cyclodextrin have shown that neither mβCD nor mβCD-chol interacted with the gold surface (not shown). Hence, gold surfaces devoid of cells or phospholipids (~30%) did not absorb cyclodextrin molecules directly.

Cell culture

HeLa cells were cultured routinely in Dulbecco's modified Eagle's medium (D-MEM, Biological Industries, Kibbutz Beit Haemek, Israel), supplemented with 4.5 g/l D-glucose, 10% antibiotics (stock solution: 10,000 units/ml penicillin, 10 mg/ml streptomycin, 0.025 mg/ml amphotericin, Biological Industries) and 10% fetal calf serum. A subconfluent cell monolayer cultured on a 10 cm plate was detached from the dish by treatment with trypsin C (0.05% Trypsin/EDTA in Puck's saline A; Biological Industries) and brought with growth medium to a density of 4×10^6 cells/ml. A drop of ~200 μl of the cell suspension was placed carefully on the center of the gold-coated prism, previously mounted on the base of a sterile Pyrex glass beaker. Cells were allowed to attach for 30 min at room temperature. Thereafter, the beaker was filled with growth medium so that it slightly exceeded the level of the gold-coated surface of the prism. The cover of a sterile petri dish was placed on top of the beaker and placed in a CO_2 incubator (5% CO_2, 37°C, 90% humidity). Cells were allowed to grow on the gold surface for 5–7 days. Under these conditions, a cell monolayer covering ~70% of the gold surface (evaluated by light microscopy) was formed. Cell monolayers with lower confluence were obtained upon decreasing the cell suspension density. An example of a cell on the Au surface on the prism is shown schematically in Fig. 2. A representative light microscopic image of HeLa cells cultured on the Au-coated prism is shown in Fig. 3 *b*.

Cholesterol depletion and enrichment

For inducing cholesterol depletion, we used mβCD (Sigma (St. Louis, MO), C-4555). This substance neither binds to nor penetrates into the plasma membrane. α-CD (Sigma, C-4642) was used as a partially inactive analog of mβCD. Before use, the cyclodextrins were dissolved in minimal essential medium (MEM) containing 20 mM HEPES pH 7.2 and Hanks' salts (GIBCO/BRL (Life Technologies), Gaithersberg, MD). For cholesterol enrichment experiments, mβCD-chol complexes were prepared as previously described (15). Briefly, 0.03 g cholesterol was mixed with 1 g of mβCD dissolved in 20 ml of water. The mixture was rotated overnight at 37°C until a clear solution was obtained. Next, the solution was freeze dried and maintained at 4°C until use. Cells or artificial POPC-decanethiol layers (see below) in the flow chamber were exposed to mβCD or mβCD-chol at 37°C. Exposure time and substance concentrations are specified in the figure legends. Cholesterol levels were determined biochemically on cells cultured at 70% confluence, using the Infinity cholesterol reagent kit (Sigma, 402-20). Cholesterol levels were normalized to cellular protein determined by the BCA (bicinchoninic acid) protein assay (Pierce Biotechnology, Rockford, IL). Schematic illustration of cyclodextrin-mediated cholesterol depletion or enrichment is presented in Fig. 2.

Generation of the POPC-decanethiol hybrid layer

The assembly of a POPC monolayer over a decanethiol gold-coated surface was performed as described previously (16).

Electron microscopy

HeLa cells were cultured on plastic culture dishes and processed according to the method of Orzech et al. (17).

RESULTS

FTIR-SPR measurements on living HeLa cells

The FTIR-SPR setup is described in the Materials and Methods section and in Fig. 1, upper panel. It permits studying the SPR reflectivity (R) versus the wavelength (λ) for different external angles, θ. Representative $R(\lambda)$ curves measured at different fixed θ values for the Au/air interface are depicted in Fig. 1, middle panel. Each curve is characterized by a clear minimum, λ_{min}, whose position depends on θ. Three-dimensional plots of $R(\lambda, \theta)$ can be constructed from experimental data for SPR reflectivity versus λ at different

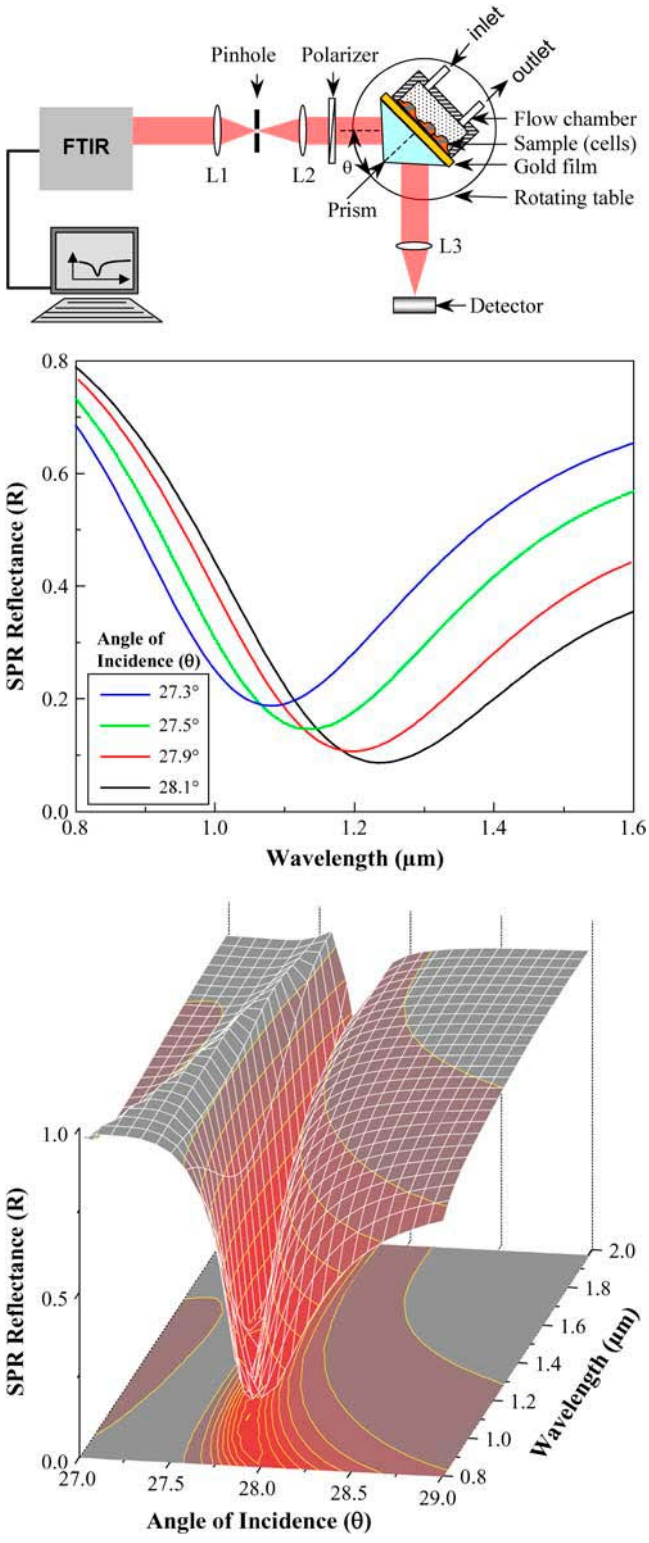

FIGURE 1 FTIR-SPR experimental setup. (*Upper panel*) Living cells were cultured onto a thin metallic (gold) film that coated a glass prism. The sample was illuminated with a collimated polarized IR light beam emitted from the FTIR spectrometer. During the measurements, the cells were in continuous contact with growth medium that filled the flow chamber. (*Middle panel*) Representative curves of FTIR-SPR reflectivity versus wavelength for the Au/air interface and for several angles of incidence, θ (see *inset*); the Au thickness in this experiment was 34 nm. Spectra were the average of 32 scans collected at a 32 cm^{-1} resolution corresponding to the wavelength step of ~3 nm. (*Lower panel*) A three-dimensional reconstruction plot of $R(\lambda, \theta)$ for the Au/air interface shown in the middle panel. Note that at longer wavelengths the angular width of the SPR minimum becomes narrower.

values of θ (Fig. 1, *lower panel*). Vertical slices of $R(\lambda, \theta)$ allow the determination of R versus θ at fixed values of λ. For instance, Fig. 3 shows slices of $R(\theta)$ at two fixed wavelengths ($\lambda = 0.92$ μm (*panel a*) and $\lambda = 1.6$ μm (*panel b*)) for Au/medium (*cyan*) and Au/cells/medium interfaces. As shown clearly, in all cases the angular width of the SPR profile is narrower by a factor of ~10 at $\lambda = 1.6$ μm, compared with the angular width at $\lambda = 0.92$ μm.

HeLa cells were cultured on an Au-coated prism at various cell densities. Under our working conditions, adhered cells tend to form a disordered monolayer, i.e., cells were distributed inhomogeneously over the gold surface, consequently forming regions with varied cell densities (shown in the light microscopic image presented in the *inset* of Fig. 3 *b*). SPR reflectance (R), as a function of external angle (θ), measured for different cell densities revealed a double minima profile (denoted (*I*) and (*II*)) at the two excitation wavelengths, $\lambda = 0.92$ μm and $\lambda = 1.6$ μm (Fig. 3, *a* and *b*). Notably, however, at the shorter excitation wavelength the double minima shape was hardly resolved, whereas $R(\theta)$ curves of the same sample but at $\lambda = 1.6$ μm clearly resolved two narrow-shaped minima (Fig. 3 *b*). The higher resolution of the SPR spectrum at $\lambda = 1.6$ μm is due to the much narrower SPR resonances (18). This narrowing effect is even more pronounced at the mid-IR wavelength range (data not shown).

Interestingly, an increase in the SPR reflectance values of minimum I and a corresponding decrease in the reflectance of minimum II were observed upon cell culturing at increased confluence (Fig. 3 *b*). These data are consistent with the possibility that minima I and II are contributed by cell-free and cell-occupied regions on the Au film, respectively. The degree of cell confluence, P, could be determined by taking the total reflectance, R, as a sum of the form $R = (1 - P) \times R_I + P \times R_{II}$, where R_I and R_{II} are reflectivities from the empty gold, minimum I, and gold occupied by cells, minimum II, respectively. The estimated values of P are given in the inset of Fig. 3 *a*. These values were nearly identical to the cell coverage determined by light microscopic analyses, suggesting that FTIR-SPR provides a reliable estimate in real time of the degree of Au-surface occupancy.

Manipulating HeLa cell cholesterol levels resulted in shifts in the FTIR-SPR signal

We next examined whether FTIR-SPR measurements respond to alterations in HeLa cell membrane cholesterol enrichment or depletion. For that purpose, Au-cultured cells

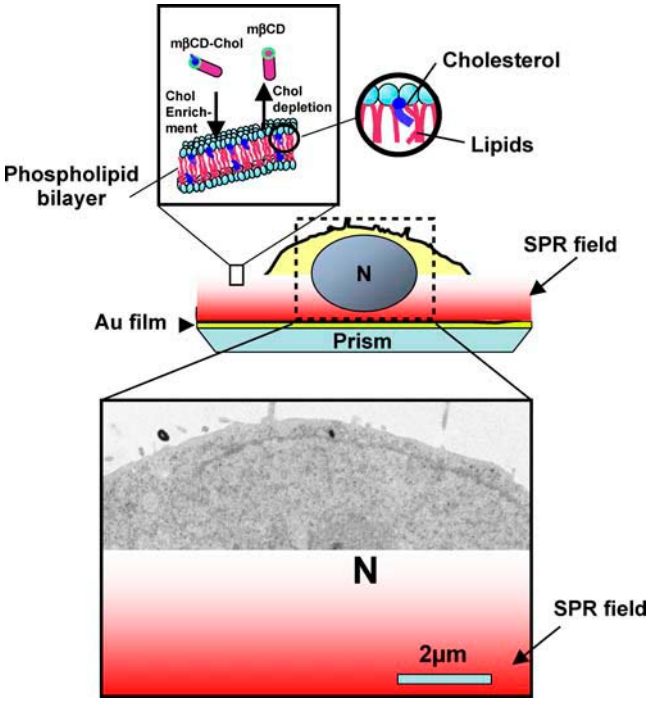

FIGURE 2 Schematic representation of cell membrane cholesterol depletion and enrichment. Cells were cultured on the gold-coated prism. Cholesterol was either extracted from or inserted into the plasma membrane of Au-cultured HeLa cells, using mβCD or mβCD saturated with cholesterol (mβCD-Chol), respectively. For analysis by electron microscopy, similar treatments were performed on cells adhered onto plastic dishes. A representative electron micrograph of untreated cell is shown. The SPR field traverses the cell-substrate interface and penetrates up to ~2 μm deep into the cell volume (schematically illustrated by a *red gradient*). ''N'' stands for nucleus.

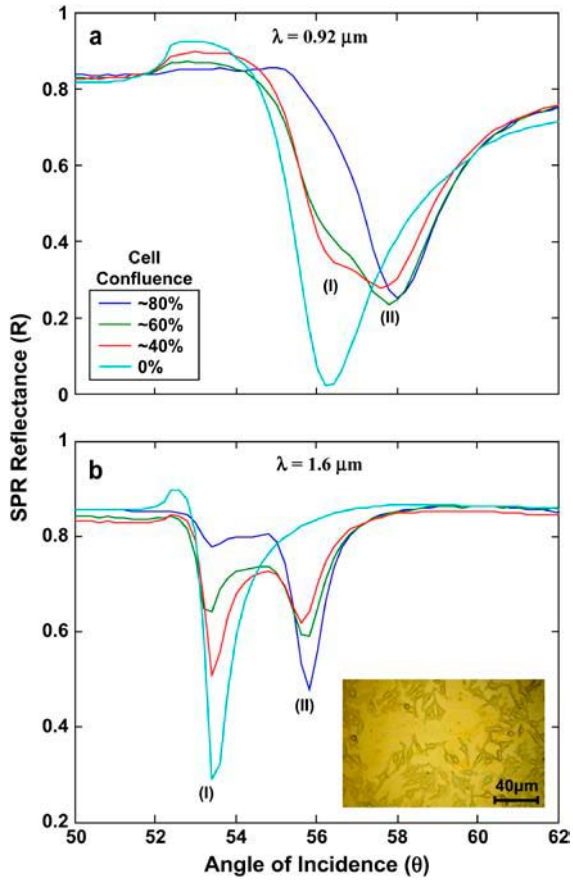

FIGURE 3 FTIR-SPR reflectance versus external angle from an Au-free or HeLa cell-occupied Au surface. Cells were cultured under conditions yielding ~80% (*blue*), ~60% (*green*), and ~40% (*red*) cell occupancy of the gold-coated surface. Zero percent refers to an empty gold-coated prism subjected to cell growth medium (*cyan*). The degree of cell confluence was quantified with respect to the surface area occupied by the cells in a given microscopic field using images taken by phase contrast microscopy. A representative image of ~40% cell coverage is shown in the inset of panel *b*. These data fully correlated with the degree of cell surface coverage estimated by FTIR-SPR scans (see text). FTIR-SPR measurements were performed at $\lambda = 0.92$ μm (*panel a*) or 1.6 μm (*panel b*). Two SPR minima denoted as (*I*) and (*II*) were seen only when the Au surface was partly occupied with cells. These minima were clearly resolved only at the higher wavelength (*panel b*).

(~70% confluence) were treated with mβCD saturated with cholesterol (mβCD-chol complex) to insert cholesterol into the plasma membrane or conversely with mβCD alone to deplete cholesterol from the cell membrane (illustrated in Fig. 2). Representative $R(\lambda)$ curves obtained immediately after introducing mβCD-chol (*green*), after cell exposure to the complex for 8 min (*blue*), and after 15 min of cell exposure to mβCD-chol followed by a 5-min wash and subsequently 7 min of mβCD treatment (i.e., a 27-min time, denoted by *red*) are shown in the upper panel of Fig. 4. Data showing λ_{min} as a function of time are depicted in the lower panel of Fig. 4. An instant exponential shift with time of the λ_{min} toward longer wavelengths was observed upon cell exposure to mβCD-chol (10 mM); λ_{min} leveled off after 5 min, suggesting that it has reached saturation (Fig. 4, *lower panel*, phase (*a*)). After 15 min of treatment, cells were washed with plain medium for an additional 5 min and then exposed to mβCD (3 mM). This induced an immediate shift in the SPR λ_{min} signal toward shorter wavelengths, reaching minimal levels after ~25 min of treatment (Fig. 4, *lower panel*, phase (*b*)). Notably, λ_{min} eventually decreased below the starting point value ($\lambda_{min} = 1.085$ μm), suggesting that cholesterol had been depleted at below the endogenous levels.

Cholesterol levels in parallel cell cultures were determined biochemically at three time points during the above experiment (data obtained are encircled in Fig. 4, *lower panel*). Nontreated cells contained 20.4 mg cholesterol per gram of cellular protein, a value consistent with previous cholesterol determinations in HeLa cells (15). Cells treated with mβCD-chol for 20 min exhibited elevated cholesterol levels up to ~25 mg cholesterol/gram protein. Subsequent treatment with mβCD for 30 min lowered the cellular cholesterol level to ~9 mg cholesterol/gram protein. These data provide empirical evidence for the expected ability of cyclodextrins to manipulate membrane cholesterol levels.

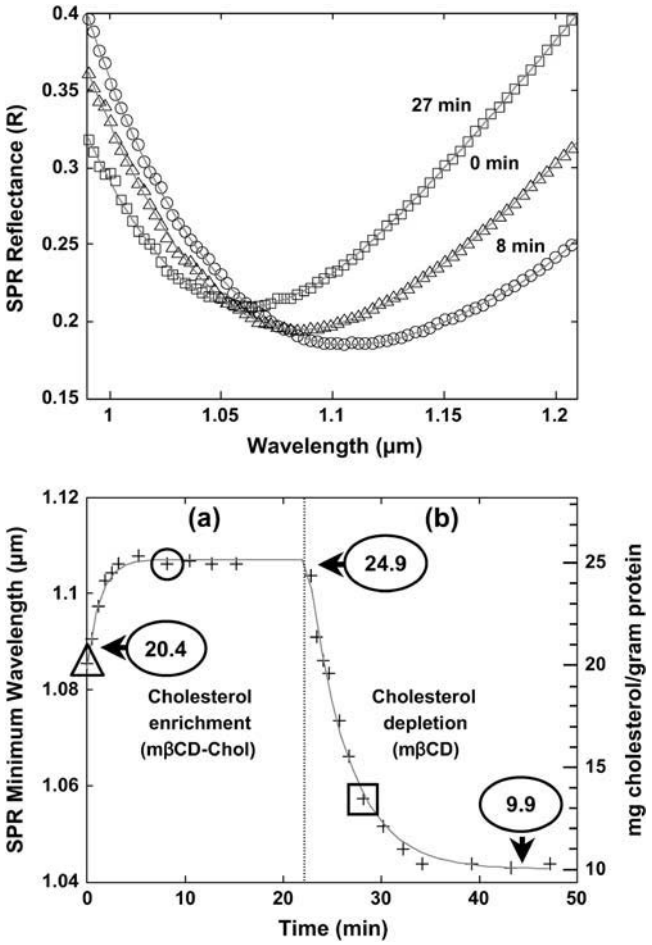

FIGURE 4 FTIR-SPR measurements on HeLa cells whose membrane cholesterol levels have been altered by cyclodextrins. (*Upper panel*) Representative examples of $R(\lambda)$ curves taken from FTIR-SPR measurements of HeLa cells cultivated at ~70% confluence. Each $R(\lambda)$ measurement was recorded using a second timescale. Measurements were performed immediately upon cell exposure to cyclodextrin treatment (0 min, △) and at times 8 min (○) and 27 min (□) after the initial injection of 10 mM mβCD-chol. The solid lines represent polynomial fits to experimental data. Values corresponding to λ_{min} were derived from similar curves taken at different times. (*Lower panel*) Summary of FTIR-SPR minimum wavelength versus time. mβCD-chol containing solution was injected into the flow cell at zero time. SPR measurements of $R(\lambda)$ commenced immediately thereafter (phase (*a*)). After ~15 min, the cells were washed with plain medium for ~5 min (no data were taken during that time) and then mβCD (3 mM, phase (*b*)) was injected into the flow cell. Cholesterol levels were determined biochemically in parallel cell cultures treated identically (encircled values, expressed as milligram cholesterol per gram cell protein). Arrows indicate the times. Crosses represent experimental data taken at a specific time. The solid line represents a best-fit analysis to the Langmuir type exponential behavior. The triangle, circle, and rectangle refer to the minima in the upper panel. Importantly, at the end of each measurement, we estimated the degree of Au coverage by cells using the SPR measurements and light microscopy. We found that the amount of cells attached to the Au support remained virtually identical (i.e., 70%) to that estimated in the beginning of the experiment.

Cyclodextrin treatments caused reversible shifts in the SPR signal

Next we investigated whether the shifts in the SPR signal respond reversibly to successive cycles of cholesterol enrichment and depletion. Initially, cells were exposed to two cycles of cholesterol enrichment (Fig. 5, *upper panel*, phases (*a*) and (*c*)), intervened with a step of cholesterol depletion (Fig. 5, *upper panel*, phase (*b*)). The SPR minimum shift increased exponentially with time in response to cholesterol enrichment, decreased upon cholesterol depletion, and increased again when subjected to a second round of cholesterol enrichment. These results suggest that shifts in the SPR signal respond consistently and as expected to cholesterol enrichment and depletion.

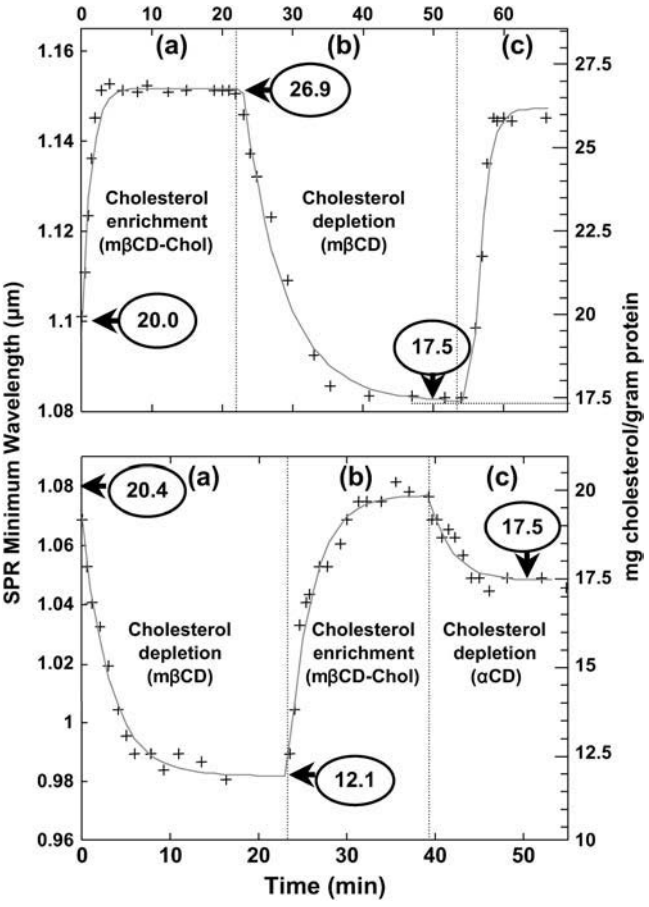

FIGURE 5 Shifts in the FTIR-SPR wavelength minima responded reversibly to cycles of cholesterol depletion and enrichment. Experiments were performed as described in Fig. 4. (*Upper panel*) Cells were exposed to two cycles of cholesterol enrichment (20 mM mβCD-chol; phases (*a*) and (*c*)) alienated by a step of cholesterol depletion (3 mM mβCD; phase (*b*)). Encircled numbers are cholesterol concentrations (milligram cholesterol/gram protein) determined biochemically on analogous cell cultures. (*Lower panel*) Cells were initially treated with mβCD (10 mM; phase (*a*)), followed by mβCD-chol (10 mM; (*b*)), and finally with the inactive analog of mβCD, αCD (3 mM; (*c*)). The various treatments did not alter significantly the degree of cell confluence (~70%) monitored before and after each measurement.

In the latter experiments, HeLa cells (cultured at 70% confluence) were exposed to a twofold higher concentration of mβCD-chol (20 mM, Fig. 5, *upper panel*). The shift in the SPR minima correspondently increased from $\lambda_{min} = 1.10$ μm, (at time zero) to plateau levels of $\lambda_{min} = 1.15$ μm. The net total difference ($\Delta\lambda_{min} = 0.05$ μm) is ~2-fold higher than that observed in cells treated with 10 mM mβCD-chol ($\Delta\lambda_{min} = 0.022$ μm; see Fig. 5, *lower panel*).

The reversible nature of the SPR signal response was also observed when cell membranes were first depleted and subsequently enriched with cholesterol (Fig. 5, *lower panel*, phases (*a*) and (*b*)). Exposure to the partially inactive analog of mβCD, α-cyclodextrin (α-CD), caused a relatively minor diminishment of the SPR signal (Fig. 5, *lower panel*, phase (*c*)), consistent with its being partially inactive. Notably, >95% of the cells were viable at the end of each experiment, as estimated by Tripan blue staining, implying that FTIR-SPR measurements did not significantly hamper cell viability.

FTIR-SPR measurements on a model phospholipid membrane

To date, all experiments were conducted on cells. It is possible that in complex systems such as cells, the cellular processes mediated in response to acute cyclodextrin treatments contributed to the observed shifts in the SPR signal. To address this hypothesis and its functional consequence, we examined the effects of cholesterol enrichment and depletion using a simpler model membrane, namely, on an artificial phospholipid (2-oleoyl-1-palmitoyl-*sn*-glycerol-3-phosphocholine (POPC)) monolayer assembled on an Au-coated prism formerly covered with a hydrophobic layer of decanethiol.

The $R(\lambda)$ curves (not shown) are in good agreement with the Fresnel model (14,19,20) and under the assumption that the lipids form a monolayer, the fit allowed us to determine an ''average'' lipid density on the Au surface (3). Upon the addition of POPC, the SPR minima shifted toward longer wavelengths (Fig. 6, phase (*a*)), reflecting the adsorption kinetics of the phospholipid molecules onto the gold-modified decanethiol surface. After ~20 min of exposure to POPC, the shift reached a saturated value, suggesting maximal coverage of the decanethiol with the POPC molecules. Under the experimental conditions employed, ~70% of the surface was covered with POPC.

Next, the constructed POPC-decanethiol hybrid layer was washed with buffer and immediately exposed to mβCD-chol. The SPR minimum shifted instantly to longer wavelengths (Fig. 6, phase (*b*)). After a brief wash with plain medium, a solution containing mβCD was injected into the flow cell. In subsequent SPR measurements we detected an exponential decrease in the SPR λ_{min} shift (Fig. 6, phase (*c*)). Interestingly, the shift decreased to the baseline level, which was contributed by the phospholipid layer, indicating that mβCD removed exclusively all inserted cholesterol molecules without affecting the POPC-decanethiol layers. This is consistent with in vitro studies showing that β-cyclodextrins neither bind nor penetrate into membranes and have a high affinity for sterols as compared to other lipids (21,22).

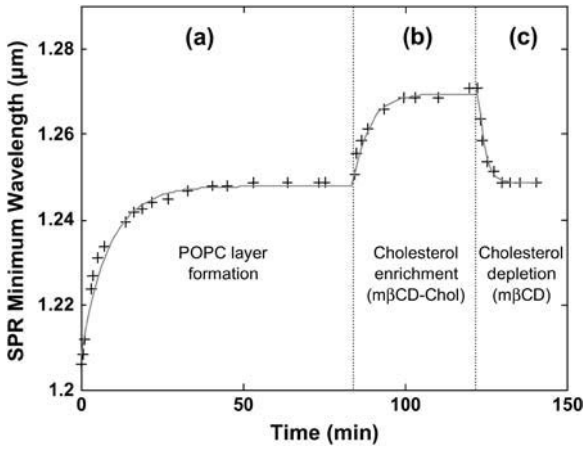

FIGURE 6 FTIR-SPR measurements on a phospholipid (POPC)-decanethiol hybrid layer. Summary of FTIR-SPR minimum wavelength versus time. Fresnel fits of $R(\lambda)$ curves (not shown) yielded an Au thickness of 28.5 nm, a decanethiol thickness of 1 nm, and a phospholipid layer thickness of 2.96 nm. In phase (*a*), measurements were performed throughout POPC membrane formation. After reaching a steady state (~70% of the gold surface was covered with the phospholipid), the monolayer was treated with mβCD-chol (10 mM for ~25 min (phase *b*)). After a brief washing with plain medium, the hybrid layer was treated with mβCD alone (3mM; phase (*c*)).

DISCUSSION

The data presented in this study indicate that FTIR-SPR measurements can serve as a useful tool for monitoring changes in cell occupancy and membrane biochemical composition. In the former case, the degree of cell occupancy could be calculated from the highly resolved narrower shaped minima observed in the $R(\theta)$ spectra at the longer excitation wavelength (Fig. 3 *b*). This feature may be further developed in future experiments for assaying cell proliferation, cell detachment, and cell death.

Our data also indicate that the FTIR-SPR signal responds to alterations in the membrane cholesterol levels. The following experimental evidence supported this conclusion: 1), Treating cells with mβCD-chol elevated the cellular cholesterol levels. 2), The same treatment also caused a time-dependent increase in λ_{min}. 3), Treatment with mβCD alone depleted cholesterol and caused changes in λ_{min}, in the opposite direction. Similar results were observed in simple POPC monolayers, suggesting that the observed SPR signal shifts in cells were contributed by the mere enrichment or depletion of membrane cholesterol. In agreement with numerous previous data (22–25), all these effects are consistent with β-cyclodextrins (unloaded or loaded with cholesterol) being efficient cholesterol shuttles. Furthermore, all these

effects were entirely reversible and ineffective upon exposure to αCD, which slightly lowered cholesterol levels and diminished the SPR signal (Fig. 5).

A conceivable scenario suggests that in the course of cholesterol enrichment, cyclodextrins loaded with cholesterol deliver their content directly into the contact-free membranes (25) (Fig. 2), where it is efficiently incorporated into the two leaflets ($t_{1/2} \sim 1$ s) of the bilayer (26,27). Cholesterol molecules are then rapidly diffused and consequently occupy the entire plane of the cell surface. Cholesterol depletion caused selective removal of cholesterol primarily from the outer leaflet of the cell plasma membrane. Since FTIR-SPR produces an evanescent wave that propagates laterally and penetrates up to ~ 2 μm into the cell interior (illustrated in Fig. 2), it is highly probable that the measurements detected changes occurring at cell surface regions that are in contact with the Au substrate, as well as in those that are contact-free, located somewhat distal to the Au substrate.

SPR measurements are highly sensitive to both dielectric properties and layer thickness. Therefore, changes in the SPR signal in response to manipulations of cholesterol levels could be contributed by changes in these two parameters. However, recent x-ray scattering experiments showed that cholesterol depletion by cyclodextrins has virtually no effect on bilayer thickness of cell membranes (13). These experimental data reinforce the possibility that the SPR shifts upon cholesterol depletion are contributed mostly by changes in dielectric properties, and not by alterations in lipid bilayer thickness. In the context of these x-ray data, we carried out Fresnel simulations on a model consisting of three layers: Au/decanethiol/POPC and an infinite layer of water placed on top of the POPC (for details see Lirtsman and Ziblat (28)). This analysis revealed that under the assumption that in cholesterol-depleted cells the SPR λ_{min} shift from 1.06 to 0.98 μm (i.e., $\sim$8%, reduction in the SPR signal; see Fig. 5, *lower panel*, phase (*a*)) is exclusively contributed by an altered dielectric constant (and not by layer changes in thickness), the phospholipid layer width would change by $\sim$4%. In contrast, simulations under the assumption that the same experimental SPR shift was contributed solely by a thickness variation yielded an unrealistic thickness decrease of $\sim$130%. These theoretical considerations may add additional support to the hypothesis that the experimental λ_{min} shift in mβCD-treated cells is contributed mostly by changes in the dielectric constant rather than bilayer thickness.

It is possible that cyclodextrin treatment resulted in changes in cell thickness that contributed to the SPR signal shift. In attempting to address this speculation, we performed a morphological analysis of mβCD-treated and -untreated cells using thin section electron microscopy (Fig. 2). Cholesterol-depleted cells revealed no significant morphological alterations compared to untreated cells (data not shown), suggesting that changes in cell shape did not contribute to the SPR signal shifts. In addition, it would be hard to envision how the same morphological changes had contributed to identical directionality in the SPR signal shifts observed in both artificial POPC-decanethiol layers and living cells.

SPR studies on viable cells have been reported recently (29). However, these studies imaged the topology of cell-substrate contacts, and to the best of our knowledge no published data exist on SPR measurements of biochemical variations in living cells. Thus, we believe that our application of the FTIR-SPR represents a significant advance in the SPR field, providing a ''proof of principle'' that SPR can be used as a label-free method to study in real time alterations in the biochemical composition of cell membranes.

SPR λ_{min} values shifted in proportion to cholesterol levels determined biochemically (Figs. 4, *lower panel*, and 5). Thus, a single biochemical determination of cholesterol concentration could be sufficient for extrapolating its cellular levels by SPR. We believe that SPR measurements are not limited to the monitoring of cholesterol. Similar measurements can be applied to investigate the activity of newly developed lipid modulators. The system can also be potentially used to sense the interactions between cells and other biomolecules whose dielectric properties facilitate their sensitive detection. For instance, our most recent measurements revealed that subtle changes in subphysiological concentrations ($\sim$0.001% w/v; 0.05 mM) of D-glucose added to pure water could be detected by FTIR-SPR measurements (data not shown). These preliminary results suggest that SPR technology can be potentially used for sensing alterations in sugar concentrations occurring within cells, e.g., during the transcellular transport of glucose across tight intestinal epithelium and in complex biochemical environments such as the blood plasma. Hence, successful development of this research avenue may contribute important new tools for studying and diagnosing diabetes.

The analytical capability of the method will be significantly enhanced when specific structural features of biomolecules are identified by SPR. Measurements at longer wavelengths (particularly those of 7–12 μm) produced SPR reflectance spectra with increased resolution, namely, with a sharper angular width, as recently demonstrated (28). This may allow the observation of different SPR lines contributed by different and specific cell organelles having different dielectric properties. In addition, the FTIR-SPR system working in the mid-IR range may also excite various vibration modes in the biological system identified as unique ''chemical fingerprints'' in the reflectance, which will contribute to the SPR signal. The detection sensitivity of these modes should be very high due to the considerable enhancement of the signal. In addition, since the decay length of the SP waves is in the order of the light excitation wavelength, the use of mid-IR excitation will produce an evanescent wave that penetrates deeper into the sample, enabling the entire cell to be examined in terms of height and volume. In this respect, we envision that future development of this technology, particularly its upscaling to the mid-IR wavelength range, may enable one to study various dynamic processes that change

the dielectric properties and thickness of the whole cell (e.g., global changes in cell volume), the cell surface (e.g., ligand-receptor interactions), or in cytoplasm (e.g., intracellular transport of amino acids and sugars). Of course, successfully performing these experiments will largely depend upon the ability of FTIR-SPR to sensitively detect changes in reflectivity contributed by the interacting molecules. Further improvement of this technology may lead to the development of novel research directions, having an important impact on the fields of the biomedical sciences and biotechnology.

We thank Prof. Yechezkel Barenholz (Dept. of Biochemistry, Hebrew University-Hadassah Medical School) and Anan Copty (Racah Institute of Physics) for helpful discussions and critical reading of the manuscript.

This work was supported in part by a grant from the DFG, Germany (D.D.) and by The Israel Science Foundation (grant No. 1337/05).

REFERENCES

1. Knoll, W. 1998. Interfaces and thin films as seen by bound electromagnetic waves. *Annu. Rev. Phys. Chem.* 49:569–638.
2. Liedberg, B., C. Nylander, and I. Lundstrom. 1995. Biosensing with surface plasmon resonance—how it all started. *Biosens. Bioelectron.* 10:i–ix.
3. Plant, A. L., M. Brigham-Burke, E. C. Petrella, and D. J. O'Shannessy. 1995. Phospholipid/alkanethiol bilayers for cell-surface receptor studies by surface plasmon resonance. *Anal. Biochem.* 226:342–348.
4. Lange, Y., M. H. Swaisgood, B. V. Ramos, and T. L. Steck. 1989. Plasma membranes contain half the phospholipid and 90% of the cholesterol and sphingomyelin in cultured human fibroblasts. *J. Biol. Chem.* 264:3786–3793.
5. van Meer, G. 1989. Lipid traffic in animal cells. *Annu. Rev. Cell Biol.* 5:247–275.
6. Simons, K., and E. Ikonen. 2000. How cells handle cholesterol. *Science.* 290:1721–1726.
7. Mouritsen, O. G., and M. J. Zuckermann. 2004. What's so special about cholesterol? *Lipids.* 39:1101–1113.
8. Barenholz, Y. 2004. Sphingomyelin and cholesterol: from membrane biophysics and rafts to potential medical applications. *Subcell. Biochem.* 37:167–215.
9. Holthuis, J. C., and T. P. Levine. 2005. Lipid traffic: floppy drives and a superhighway. *Nat. Rev. Mol. Cell Biol.* 6:209–220.
10. Hui, S. W., and N. B. He. 1983. Molecular organization in cholesterol-lecithin bilayers by x-ray and electron diffraction measurements. *Biochemistry.* 22:1159–1164.
11. Nezil, F. A., and M. Bloom. 1992. Combined influence of cholesterol and synthetic amphiphillic peptides upon bilayer thickness in model membranes. *Biophys. J.* 61:1176–1183.
12. Smondyrev, A. M., and M. L. Berkowitz. 1999. Structure of dipalmitoylphosphatidylcholine/cholesterol bilayer at low and high cholesterol concentrations: molecular dynamics simulation. *Biophys. J.* 77:2075–2089.
13. Mitra, K., I. Ubarretxena-Belandia, T. Taguchi, G. Warren, and D. M. Engelman. 2004. Modulation of the bilayer thickness of exocytic pathway membranes by membrane proteins rather than cholesterol. *Proc. Natl. Acad. Sci. USA.* 101:4083–4088.
14. Raether, H. 1988. Surface-Plasmons on Smooth and Rough Surfaces and on Gratings. Springer-Verlag, Berlin.
15. Grimmer, S., T. G. Iversen, B. van Deurs, and K. Sandvig. 2000. Endosome to Golgi transport of ricin is regulated by cholesterol. *Mol. Biol. Cell.* 11:4205–4216.
16. Granek, V., and J. Rishpon. 2002. Detecting endocrine-disrupting compounds by fast impedance measurements. *Environ. Sci. Technol.* 36:1574–1578.
17. Orzech, E., S. Cohen, A. Weiss, and B. Aroeti. 2000. Interactions between the exocytic and endocytic pathways in polarized Madin-Darby canine kidney cells. *J. Biol. Chem.* 275:15207–15219.
18. Brink, G., H. Sigl, and E. Sackmann. 1995. Near-infrared surface plasmon resonance in silicon-based sensor: new opportunities in sensitive detection of biomolecules from aqueous solutions by applying microstep for discriminating specific and non-specific binding. *Sens. Actuators B. Chem.* 24–25:756–761.
19. Born, M., and E. Wolf. 1980. Principles of Optics, 6th ed. Pergamon, Oxford.
20. Windt, D. L. 1998. IMD-software for modeling the optical properties of multilayer films. *Comput. Phys.* 12:360–370.
21. Irie, T., K. Fukunaga, and J. Pitha. 1992. Hydroxypropylcyclodextrins in parenteral use. I: Lipid dissolution and effects on lipid transfers in vitro. *J. Pharm. Sci.* 81:521–523.
22. Ohtani, Y., T. Irie, K. Uekama, K. Fukunaga, and J. Pitha. 1989. Differential effects of alpha-, beta- and gamma-cyclodextrins on human erythrocytes. *Eur. J. Biochem.* 186:17–22.
23. Christian, A. E., M. P. Haynes, M. C. Phillips, and G. H. Rothblat. 1997. Use of cyclodextrins for manipulating cellular cholesterol content. *J. Lipid Res.* 38:2264–2272.
24. Kilsdonk, E. P., P. G. Yancey, G. W. Stoudt, F. W. Bangerter, W. J. Johnson, M. C. Phillips, and G. H. Rothblat. 1995. Cellular cholesterol efflux mediated by cyclodextrins. *J. Biol. Chem.* 270:17250–17256.
25. Yancey, P. G., W. V. Rodrigueza, E. P. Kilsdonk, G. W. Stoudt, W. J. Johnson, M. C. Phillips, and G. H. Rothblat. 1996. Cellular cholesterol efflux mediated by cyclodextrins. Demonstration of kinetic pools and mechanism of efflux. *J. Biol. Chem.* 271:16026–16034.
26. Steck, T. L., J. Ye, and Y. Lange. 2002. Probing red cell membrane cholesterol movement with cyclodextrin. *Biophys. J.* 83:2118–2125.
27. Muller, P., and A. Herrmann. 2002. Rapid transbilayer movement of spin-labeled steroids in human erythrocytes and in liposomes. *Biophys. J.* 82:1418–1428.
28. Lirtsman, V., and R. Ziblat, M. Golosovsky, D. Davidov, R. Pogreb, V. Sacks-Granek, and J. Rishpon. 2005. Surface-plasmon-resonance with infrared excitation: studies of phospholipid membrane growth. *J. Appl. Phys.* 98:1–6.
29. Giebel, K., C. Bechinger, S. Herminghaus, M. Riedel, P. Leiderer, U. Weiland, and M. Bastmeyer. 1999. Imaging of cell/substrate contacts of living cells with surface plasmon resonance microscopy. *Biophys. J.* 76:509–516.